European Journal of Pharmaceutical Sciences 175 (2022) 106229

Contents lists available at ScienceDirect

European Journal of Pharmaceutical Sciences

journal homepage: www.elsevier.com/locate/ejps

Mucoadhesive meloxicam-loaded nanoemulsions: Development, characterization and nasal applicability studies

Bence Sipos [a], Ildikó Csóka [a], Nimród Szivacski [a], Mária Budai-Szűcs [a], Zsuzsanna Schelcz [b], István Zupkó [b], Piroska Szabó-Révész [a], Balázs Volk [c], Gábor Katona [a,*]

[a] Faculty of Pharmacy, Institute of Pharmaceutical Technology and Regulatory Affairs, University of Szeged, Eötvös Str. 6, Szeged H-6720, Hungary
[b] Faculty of Pharmacy, Institute of Pharmacodynamics and Biopharmacy, University of Szeged, Eötvös Str. 6, Szeged H-6720, Hungary
[c] Directorate of Drug Substance Development, Egis Pharmaceuticals PLC., Keresztúri Str. 30–38, Budapest H-1106, Hungary

ARTICLE INFO

Keywords:
Nasal drug delivery
Nanoemulsion
Permeation enhancement
Factorial design
Mucoadhesion
Meloxicam

ABSTRACT

Intranasally administered non-steroidal anti-inflammatory drugs (NSAIDs) offer an innovative opportunity in the field of pain management. Combination of the nasal physiological advantages such as the rich vascularization and large absorption area along with novel nanomedical formulations can fulfill all the necessary criteria of an advanced drug delivery system. Nanoemulsions represent a versatile formulation approach suitable for nasal drug delivery by increasing the absorption and the bioavailability of many drugs for systemic and nose-to-brain delivery due to their stability, small droplet size and optimal solubilization properties. In this study we aimed to develop meloxicam (MX)-loaded mucoadhesive nanoemulsions and to investigate the nasal applicability of the optimized formulations. Our results indicated the optimized nanoemulsion formulation (MX-NE3) had a droplet size of 158.5 nm in monodisperse droplet size distribution (polydispersity index of 0.211). The surface charge was −11.2 mV, which helped with the colloidal stability upon dilution at simulated nasal conditions and storage. The high encapsulation efficiency (79.2%) mediated a 15-fold drug release and a 3-fold permeability increase at nasal conditions compared to the initial MX. Proper wetting properties associated with high mucoadhesion prosper the increased residence time on the surface of the nasal mucosa. No cytotoxic effect of the formulations was observed on NIH/3T3 mouse embryonic fibroblast cell lines, which supports the safe nasal applicability.

1. Introduction

Current drug formulation strategies focus on the improvement of the bioavailability of non-steroidal anti-inflammatory drugs (NSAIDs) as they are one of the most commonly applied groups of active substances. With oral administration, many side effects can arise due to their high dosage induced by low water solubility, leading to poor permeability through the gastrointestinal tract. Through the intranasal route, higher effective blood concentrations can be achieved (Szabó-Révész, 2018; Sipos et al., 2021a). Nasal administration has numerous advantages such as the highly vascularised nasal mucosa, the large absorption surface and the convenient applicability. The nasal pathway also provides a possibility to avoid the first-pass elimination mechanisms and a rapid onset of action is awaited by this route of administration. NSAIDs have a poor water solubility and dissolution rate at the nasal mucosa, therefore, the development of a proper drug delivery system is required, which can improve bioavailability. The main challenge is to overcome the rapid elimination from the nasal cavity due to the mucociliary clearance, which can be slowed down by application of mucoadhesive formulations.

The advantageous properties of nanoemulsions may satisfy these needs, especially if intranasal administration is selected as one of the alternative administration routes. Their main potential is that hydrophobic drugs can be incorporated in these systems, which facilitates the increased drug permeation through biological membranes and with spontaneous association tendencies they can be easily redispersed into a homogenous, administrable liquid form (Marzuki et al., 2019; Shaker et al., 2019; Choudhury et al., 2019). Furthermore, the nanoemulsion formulations may stand out due to the significant increase in mucoadhesivity and residence time.

Oil-in-water (O/W) emulsions are highly recommended for nasal application as these types of emulsions protect the drug from enzymatic and pH-mediated degradation (Bonferoni et al., 2019). The proper selection of emulsion-forming excipients plays a crucial role in designing a

* Corresponding author.
E-mail address: katona.gabor@szte.hu (G. Katona).

https://doi.org/10.1016/j.ejps.2022.106229
Received 17 March 2022; Received in revised form 10 May 2022; Accepted 31 May 2022
Available online 1 June 2022

value-added intranasal nanoemulsion. As the oily phase of the nanoemulsions, castor oil can be a suitable choice. Besides the favourable viscosity and other rheological characteristics, this natural oil can be safely applied intranasally. Furthermore, intranasal application of castor oil locallystimulates blood flow of the mucosa, which helps with the permeability of the active substance (Espinoza et al., 2018). As surfactant Tween 80 seems to be a rational choice as it forms O/W type emulsions (HLB value = 15), moreover it has low toxicity and irritability on the nasal mucosa (Gao et al., 2019). Besides surfactants, cosurfactants as surface-active components that co-adsorb to oil–water interfaces play a crucial role in altering interfacial characteristics, such as optimum curvature, interfacial tension, interfacial rheology, thickness, polarity, and charge. These changes in interfacial characteristics lead to changes in the formation and stability of nanoemulsions (Rao and McClements, 2013). As cosurfactant the use of propylene-glycol can be advantageous in order to solubilize the active pharmaceutical ingredient (API) and it is also able to decrease nasal irritation. To modify the bulk physicochemical and structural properties of aqueous solutions, the presence of cosolvents as water–miscible components (e.g., ethanol) are required. Ethanol as a cosolvent has the function to increase degree of dispersion of emulsified droplets through decreasing interfacial tension of the system (Rao and McClements, 2013). Moreover, ethanol is a frequently applied preservative agent in nasal drops and sprays, whereas the aqueous phase of the nanoemulsion consists of purified water (Sari et al., 2015; Prasetyo et al., 2018).

Our research group has already proved on many occasions the successful nasal application of meloxicam (MX), a member of NSAID active substance group. Horváth et al. (2016) and Bartos et al. (2018)developed MX-containing mucoadhesive nasal sprays with hyaluronic acid, while Sipos et al. (2020) designed MX-loaded polymeric micelles with rapid drug dissolution. However, in present study we are focusing on the optimization of a suitable nasal carrier system with advanced drug release property, which may assist in enhancing the bioavailability, even after absorption into the systemic circulation and reduce the need for frequent administration to improve patient compliance (Sipos et al., 2021b). Katona et al. already developed MX-human serum albumin nanoparticles with sustained nasal release, but these formulations can be stored only in solid, freeze-dried form and should be redispersed in water before use (Katona et al., 2020, 2021). The nasal delivery of NSAIDs have also shown that by nasal administration, not only analgesia, but the treatment of different chronic neurodegenerative diseases can be also accomplished. With nose-to-brain delivery through the entorhinal cortex (innerved by the olfactory nerves, too), favourable cyclooxygenase inhibition can be possible to provide a remedy to neuroinflammation in Alzheimer's Disease as well. This was supported by the rapid and more efficient brain uptake studies with ibuprofen, flurbiprofen and indomethacin as well (Parepally et al., 2006).

To satisfy these requirements, we aimed to develop a stable and dilutable MX-loaded nanoemulsion formulation as liquid dosage form with optimised droplet size and size distribution for intranasal use. Dilutable nanoemulsions are potent drug delivery vehicles for nasal use due to their numerous advantages such as increased drug release and high ability of drug penetration into the deeper layers of the nasal mucosa. The rheological characterization and the *in vitro* studies helped to determine which formulation composition was optimal for this administration route. Stability studies were carried out to determine the droplet size and droplet size distribution upon dilution at nasal conditions and storage. Drug release and permeability studies were performed to characterize the enhancement effect on these biopharmaceutical parameters mediated by the solubilization. Cell line studies on NIH/3T3 mouse embryonic fibroblasts helped to investigate the cytotoxic effect of the nanoemulsion formulations.

2. Materials and methods

2.1. Materials

Meloxicam (MX, 4-hydroxy-2-methyl-*N*-(5-methyl-2-thiazolyl)−2*H*-benzothiazine-3-carboxamide-1,1-dioxide) was kindly donated by EGIS Pharmaceuticals Plc. (Budapest, Hungary). Tween 80, castor oil, ethanol, phosphate buffered saline (PBS) powder, chemicals for Simulated Nasal Electrolyte Solution (SNES) (8.77 g/l sodium chloride (NaCl), 2.98 g/l potassium chloride (KCl), 0.59 g/l anhydrous calcium chloride ($CaCl_2$) dissolved in purified water, pH set to 5.6 1 n hydrochloride acid), potassium dihydrogen phosphate (KH_2PO_4) and the analytical grade solvent acetonitrile (MeCN) were purchased from Merck Ltd. (Budapest, Hungary). Sodium hyaluronate (HA) (MW: 4350 kD) was obtained from Gedeon Richter Plc. (Budapest, Hungary). Distilled water was purified using the Millipore Milli-Q® (Merck Ltd., Budapest, Hungary) Gradient Water Purification System.

2.2. Formulation process of MX-loaded nanoemulsions

At first, oil phase and aqueous phase were prepared separately on magnetic stirrers based on the design of experiment process. Oil phase consisted of ethanol and castor oil mixture, in which MX was dissolved under constant stirring (25 °C, 1000 rpm), while the aqueous phase contained the mixture of Tween 80, propylene glycol and purified water prepared under same conditions (25 °C, 1000 rpm). The next step was to add the oil phase into the aqueous phase using a peristaltic pump with a flow rate of 0.2 ml/min. After this, purified water was added to the mixture at a flow rate of 0.3 ml/min to form a nanoemulsion, then the system was kept under constant stirring at 25 °C for 1 h. The precise amounts later discussed were chosen based on the results of the Box-Behnken factorial design.

2.3. Optimization of MX-loaded nanoemulsions

To optimize the formulation of MX-loaded nanoemulsions, a 4-factor, 3-level Box-Behnken factorial design was set up. Generally speaking, the formulation process is scalable and can produce large amounts of nanoemulsions. The formulation strategy is affected by the drop rate of oily phase to the aqueous phase, however laboratory scale process and industrial scale-up is influenced by the ratio of the components (Singh et al., 2017). The simplicity of this method lies in the fact that by utilizing the self-association tendency of these specific components, high pressure or energy conditions are not required to form colloidally stable and proper nanoemulsion droplets. Based on literature data and preliminary experiments, compositions from the nanoemulsion regions were selected containing Tween 80, propylene glycol, ethanol, purified water and castor oil. The independent variables with the ranges were the following (Table 1).

The concentration of MX was constant during the experiments: 0.2% w/w and for the castor oil, a permanent 3% w/w was chosen. The dependent variables were the droplet size and the polydispersity index (PdI) as the main factors influencing the dissolution and permeability rate from a nanocarrier. The effect on droplet size and PdI values was investigated by analysing the quadratic response surface and by con-

Table 1
Independent variables of the 4-factor, 3-level Box-Behnken factorial design.

	Levels		
	−1	0	+1
Independent variables	**Amount of independent variables (g)**		
Tween 80	1.20	1.60	2.0
Propylene glycol	0.75	1.00	1.25
Ethanol	0.75	1.00	1.25
Purified water	0.75	1.00	1.25

structing a second-order polynomial model using the TIBCO Statistica® 13.4 (Statsoft Hungary, Budapest, Hungary) software. The relationship of the variables on the response was described with the following second order equation (Eq. (1)):

$$Y = \beta_0 + \beta_1 x_1 + \beta_a x_1^2 + \beta_2 x_2 + \beta_b x_2^2 + \beta_3 x_3 + \beta_c x_3^2 + \beta_4 x_4 + \beta_d x_4^2 \quad (1)$$

where Y represents the response variables (droplet size and polydispersity index) of fitted surface, β_0 is a constant, β_1, β_2, β_3, β_4 are linear coefficients and β_a, β_b, β_c, β_d are quadratic coefficients of the four investigated factors. Analysis of variance (ANOVA) was applied as statistics, with a 95% confidence interval level where the variable was considered significant if the $p < 0.05$.

2.4. Characterization of MX-loaded nanoemulsions

2.4.1. Dynamic light scattering (DLS) and zeta potential measurements

The droplet size and droplet size distribution (as PdI) were measured via dynamic light scattering using a Malvern Nano ZS Zetasizer (Malvern Instrument, Malvern, UK). The formulations were measured at 25 °C with the refractive index of 1.72. The zeta potential was also measured. All measurements were performed in triplicate using a folded capillary cell. The results are expressed as means ± SD.

2.4.2. Determination of encapsulation efficiency

The content of MX entrapped in the droplets of nanoemulsion (EE%) was assayed with HPLC. In brief, the formulations were centrifuged for 1 h at 4 °C and 16,000 rpm in a Hermle Z323K laboratory centrifuge (Hermle AG, Gossheim, Germany). The amount of unentrapped MX was determined in the underneath aqueous phase (Chou et al., 2021). The EE % was calculated with the following equation (Eq. (2)):

$$EE\% = \frac{(A_1 - A_2)}{A_1} x\ 100 \quad (2)$$

where A_1 is the total MX amount (mg), A_2 is the free MX amount (mg) in the formulation. The measurements were carried out in triplicate. Results are expressed as means ± SD.

2.4.3. Quantitative analysis of MX using liquid chromatography

To determine the MX concentration during the measurements, an Agilent 1260 Infinity HPLC system (Agilent Technologies, Santa Clara, CA, USA) was used. The stationary phase was a C18 Kinetex® EVO C18 LC column (50 μm, 110 Å, 150 mm × 4.6 mm) Phenomenex, Torrance, CA, USA). The mobile phases were the following: 0.065 M KH_2PO_4 solution with adjusted pH of 2.8 with phosphoric acid (A) and methanol (B). Gradient elution was used for the separation in two steps. At first, the proportion of starting 50% A eluent was reduced to 25% over a period of 14 min and then raised again to 50% over a period of 20 min. The sample volume was 10 μl. The temperature was set at 30 °C. The eluent flow rate was set at 1 ml/min and the chromatograms were detected at 355 ± 4 nm using an UV–vis diode array detector. The data were evaluated using the ChemStation B.04.03. Software (Agilent Technologies, Santa Clara, CA, USA). The retention time of MX was 14.34 min. The linear regression of the used calibration line was 0.999. The determined limit of detection (LOD) and quantification (LOQ) were 16 and 49 ppm, respectively.

2.4.4. Determination of pH

The pH values of the formulations were measured by a dipping pH meter (WTW® inoLab® pH 7110 laboratory pH tester, Thermo Fischer Scientific, Budapest, Hungary). The measurements were carried out in triplicate. Results are expressed as means ± SD.

2.5. Rheological characterization

2.5.1. Viscosity measurements

The viscosity of the nanoemulsions was measured with a Physica MCR 302 rheometer (Anton Paar, Graz, Austria). The measuring device was of cone and plate type (diameter: 50 mm, gap height in the middle of the cone: 0.045 mm). Flow curves of the emulsions were plotted from 0.1 to 100 1/s shear rate. The viscosity of the sample was determined at 50 1/s shear rate using the interpolation function of the RheoCompass software of the instrument. Three parallel measurements were performed. Results are expressed as means ± SD.

2.5.2. Mucoadhesion study

Tensile tests were performed with a TA-XT Plus Texture analyser (Metron Ltd., Budapest, Hungary) equipped with a 5 kg load cell and a cylinder probe with a diameter of 1 cm. Nanoemulsions were placed in contact with a filter paper disc with 25 mm diameter wetted with 50 μl of an 8% w/w porcine mucin (Mucin type III, Merck Ltd., Budapest, Hungary) dispersion in SNES (pH 5.6). 20 μl of the nanoemulsions was attached to the filter paper fixed on cylinder probe and placed in contact with the mucin dispersion. A 2500 mN preload was used for 3 min, then the cylinder probe with the nanoemulsion was moved upwards at a prefixed speed of 2.5 mm × min^{-1} to separate the attaching surfaces. Adhesive force (F, mN) and adhesive work (A, mN × mm) were applied for the evaluation of the mucoadhesivity of the nanoemulsions. Five parallel measurements were performed. Results are expressed as means ± SD.

2.5.3. Determination of spreading properties via contact angle determination

Contact angles for the MX-loaded nanoemulsions on a hydrophobic substrate were measured with an OCA Contact Angle System (DataPhysics OCA 20, DataPhysics Instruments GmbH, Filderstadt, Germany). The measured contact angles were recorded every 6 s up until 1 min. Solid paraffin film was chosen as the solid substrate to investigate the wettability against a hydrophobic surface imitating the apical side of the nasal mucosa. 25 μl of the formulations was dropped with a pipette onto the surface. The measurements took place in triplicate and the results are expressed as means ± SD.

2.6. Stability studies

2.6.1. Physical stability

The optimized MX-loaded nanoemulsions were stored at ambient temperature for 4 weeks. The sampling was performed at every 7th day. At each measurement time, a portion was diluted 10-fold with purified water, then droplet size and PdI were measured using DLS. The measurements took place in triplicate and the results are expressed as means ± SD.

2.6.2. Dilution stability

Dilution stability refers to the stability of the nanoparticles upon volume expansion. The droplet size, PdI and zeta potential values were recorded in two different media: pH 5.6 SNES and pH 7.4 PBS. The rates of dilution were the following: 1, 2, 5, 10, 25 and 50. The measurements were carried out in triplicate. Results are expressed as means ± SD.

2.7. In vitro nasal applicability studies

2.7.1. In vitro nasal drug release study

The modified paddle method was used to determine the dissolution rate of the MX-loaded nanoemulsions in a Hanson SR8 Plus (Teledyne Hanson Research, Chatsworth, CA, USA) equipment. The nanoemulsions were placed in dialysis bags (Spectra/Por® Dialysis Membrane with a 12–14 kD MWCO (Spectrum Laboratories Inc., Rancho Dominguez, CA, USA). 100 ml of SNES was used as the dissolution media, measurement

was carried out at 35 °C under 100 rpm paddle rotation. At predetermined time points, 0.5 ml of aliquots were taken up to 60 min and placed in vials for the HPLC quantification measurements. Three parallel measurements took place. Results are expressed as means ± SD.

2.7.2. Model-independent statistical analysis of the drug release study

Model-independent statistical analysis of the drug release study was performed to evaluate mathematically the differences between the drug release profile of the formulations (Sipos et al., 2020). The percentage dissolution efficiency (%DE) for MX and for each MX-loaded nanoemulsion was calculated as the percentage ratio of the area under the dissolution curve up to time t to that of the area of the rectangle described by 100% dissolution at the same time as described in the following equation:

$$\%DE = \frac{\int_0^t y \cdot dt}{y_{100} \cdot t} \cdot 100\% \quad (3)$$

Trapezoidal method was used to calculate the area under the curve (AUC) which is the sum of all the trapezia defined by Eq. 4:

$$AUC = \sum_{i=1}^{i=n} \frac{(t_1 - t_{i-1})(y_{i-1} + y_i)}{2} \quad (4)$$

where t_i is the time point and y_i is the percentage of product dissolved MX at time t_i.

The relative dissolution at 15 min ($RD_{15\ min}$) in the case of the formulations compared to the inital MX was calculated based on the percentage dissolution efficacy (%DE) ratio of MX-nanoemulsion (MX-NE) and initial MX using the following formula (Eq. (5)):

$$RD_{15\ min} = \frac{\%DE_{15\ min}MX - NE}{\%DE_{15\ min}MX} \quad (5)$$

The mean dissolution time (MDT) was calculated using this expression (Eq. (6)):

$$MDT = \frac{\sum_{i-1}^{n} t_{mid}\Delta M}{\sum_{i-1}^{n} \Delta M} \quad (6)$$

where i is the dissolution sample number, n is the number of dissolution times, t_{mid} is the time at the midpoint between times t_i and t_{i-1} and ΔM is the amount of MX dissolved (mg) between times t_i and t_{i-1}.

2.7.3. In vitro nasal diffusion study

The *in vitro* nasal diffusion study of MX was performed in a modified Side-Bi-Side®-type horizontal diffusion cell, where a cellulose membrane impregnated with isopropyl myristate was applied with a surface of 0.785 cm^2. Both donor and acceptor cell volumes were 9.0 ml among which the diffusion was investigated at 35 °C. The donor phase consisted of SNES and the acceptor phase was a pH 7.4 PBS. Sampling from the acceptor phase was performed at assigned time points and the MX concentration was measured via HPLC. The aliquot volumes were 50 µl. The flux (J) was calculated from the quantity of MX permeated through the membrane, divided by the surface membrane insert and the duration of experiment (µg/cm^2/h). The permeability coefficient (K_p (cm/h)) was determined from J and the drug concentration in the donor phase (C_d (µg/cm^3)) as seen in the following equation

$$K_p = \frac{J}{C_d} \quad (7)$$

2.7.4. In vitro cytotoxicity assay

Antiproliferative effect of the samples was determined *in vitro* using NIH/3T3 mouse embryonic fibroblast cells by means of MTT [3-(4,5-dimethylthiazol-2-yl)-2,5-diphenyltetrazolium bromide] assay. Briefly, a limited number of NIH/3T3 cells (5000/well) was seeded onto a 96-well microplate and became attached to the bottom of the well overnight. On the second day of the procedure, the test substances were added in serial dilutions (final concentrations were: 0.3, 1.0, 3.0, 10.0, 30.0, 100 µM MX). After an incubation period of 72 h, the living cells were assayed by the addition of 20 µl of 5 mg/ml MTT solution. After a 4-h incubation, the medium was removed and the precipitated formazan was dissolved in 100 µl/well of DMSO during a 30-min period of shaking. Finally, the reduced MTT was assayed at 545 nm, using a microplate reader. Untreated cells were taken as the negative control. NIH/3T3 cell line was purchased from the European Collection of Cell Cultures (Salisbury, UK) and cultured in Eagle's Minimum Essential Medium. All *in vitro* experiments were carried out on two 96-well dishes with at least five parallel wells. Results are expressed as means ± SD.

3. Results and discussion

3.1. Optimization of MX-loaded nanoemulsions

During the Box-Behnken factorial design-based optimization process, 27 formulations were prepared in triplicate and the droplet size and the polydispersity index were measured. The compositions and the resulting responses can be found in Table 2.

Using the software, polynomial equations were generated to describe the effect of the independent factors on droplet size (Eq. (8)) and PdI (Eq. (9)).

$$\text{Droplet size} = 406.609 + 185.403x_1 - 168.032x_1^2 - 47.798x_2 + 88.277x_2^2 + 90.442x_3 + 53.734x_3^2 + 164.680x_4 - 123.186x_4^2 \quad (8)$$

In the case of Eq. (8), the regression coefficient (R^2) of the surface plot was 0.9983, the adjusted R^2 was 0.9912, which indicates a proper correlation. The amount of Tween 80 (x_1) had a significant ($p < 0.05$) effect on the droplet size. The positive coefficients before each independent variable indicate the increase in droplet size (x_1, x_2^2, x_3, x_3^2 and x_4) whilst the negative ones indicate the decrease (x_1^2, x_2 and x_4^2). Average nanoemulsion droplet size ranges from 100 to 300 nm and later the formulations were considered good if their droplet size fitted in this region.

$$\text{PdI} = 0.551 + 0.013x_1 - 0.1339x_1^2 - 0.068x_2 + 0.007x_2^2 + 0.051x_3 - 0.007x_3^2 + 0.122x_4 - 0.032x_4^2 \quad (9)$$

In the case of Eq. (9), the regression coefficients were 0.9941 (R^2) and 0.9897 (adjusted R^2) also indicating a proper correlation. The amount of Tween 80 (x_1^2) and purified water (x_4) had a significant ($p < 0.05$) effect on the polydispersity index. The positive coefficients before the independent variables increase the polydispersity index (x_1, x_2^2, x_3 and x_4) whilst the negative ones decrease it (x_1^2, x_2, x_3^2 and x_4^2). The formulations were considered good in droplet size distribution if the PdI value was below 0.3.

Based on the experiments and the selection of statistically significant factors (Tween 80 and purified water), 2D surface plots were depicted as seen in Fig. 1.

Based on the surface plots and the ANOVA statistical analysis, the following 4 formulations were chosen to be further investigated (Table 3). The amount of Tween 80 and purified water remained the same based on the 2D surface plots, while the other amounts would vary. The targeted castor oil concentration still remained at around 3% w/w and the targeted MX concentration was at 0.2% w/w.

The concentration of ethanol and propylene glycol in the nanoemulsions was in the range of 0.163–0.282 mg/ml and 0.146–0.233 mg/ml, respectively which means the administration of the maximal nasal applicable volume of nanoemulsions (200 µl) would be still safe for the patient. Ethanol less than 6 mg/kg/day can be safely administered for adult patients is not be expected to produce a blood alcohol concentration. In toxicological studies after long-term repeat-dose exposure (mainly by oral route), propylene glycol had a rather low systemic toxicity in experimental adult animals at up to 1 to 3 g/kg/day.

Table 2
Composition of the Box-Behnken factorial design with the measured droplet size and polydispersity index values. Fixed values: castor oil (3% w/w) and MX (0.2% w/w). Data are presented as means ± SD ($n = 3$).

Run	Tween 80 (g)	Propylene-glycol (g)	Ethanol (g)	Purified water (g)	Z-average* (nm)	PdI*
1	1.2	1.0	0.75	1.0	163.1 ± 11.3	0.514 ± 0.086
2	2.0	1.0	0.75	1.0	304.2 ± 16.4	0.463 ± 0.024
3	1.2	1.0	1.25	1.0	89.96 ± 5.3	0.455 ± 0.101
4	2.0	1.0	1.25	1.0	123.9 ± 11.7	0.459 ± 0.039
5	1.6	0.75	1.0	0.75	150.5 ± 7.3	0.271 ± 0.026
6	1.6	1.25	1.0	0.75	114.2 ± 3.0	0.338 ± 0.075
7	1.6	0.75	1.0	1.25	223.0 ± 8.4	0.337 ± 0.014
8	1.6	1.25	1.0	1.25	221.2 ± 1.8	0.384 ± 0.022
9	1.6	1.0	1.0	1.0	190.8 ± 15.5	0.308 ± 0.015
10	1.2	1.0	1.0	0.75	110.7 ± 31.7	0.525 ± 0.087
11	2.0	1.0	1.0	0.75	1217.6 ± 75.4	0.553 ± 0.041
12	1.2	1.0	1.0	1.25	1451.8 ± 261.2	0.808 ± 0.069
13	2.0	1.0	1.0	1.25	1307.4 ± 21.7	0.680 ± 0.048
14	1.6	0.75	0.75	1.0	225.2 ± 18.8	0.357 ± 0.021
15	1.6	0,75	1.25	1.0	231.5 ± 9.1	0.236 ± 0.017
16	1.6	1.25	0.75	1.0	158.5 ± 6.4	0.211 ± 0.023
17	1.6	1.25	1.25	1.0	257.4 ± 8.6	0.268 ± 0.041
18	1.6	1.0	1.0	1.0	192.5 ± 13.5	0.338 ± 0.051
19	1.2	0.75	1.0	1.0	184.4 ± 10.4	0.661 ± 0.035
20	2.0	0.75	1.0	1.0	101.2 ± 3.7	0.639 ± 0.069
21	1.2	1.25	1.0	1.0	74.71 ± 2.1	0.671 ± 0.146
22	2.0	1.25	1.0	1.0	1245.6 ± 101.9	0.879 ± 0.048
23	1.6	1.0	0.75	0.75	192.0 ± 4.9	0.362 ± 0.017
24	1.6	1.0	1.25	0.75	165.4 ± 4.5	0.251 ± 0.045
25	1.6	1.0	0.75	1.25	354.3 ± 37.1	0.698 ± 0.091
26	1.6	1.0	1.25	1.25	259.1 ± 44.8	0.432 ± 0.050
27	1.6	1.0	1.0	1.0	239.7 ± 18.3	0.346 ± 0.063

Information in juvenile animals showed that propylene glycol produces ethanol-like apoptotic neurodegeneration in the developing central nervous system of the mouse started only above doses of 2 g/kg. Langston et al. studied the long-term effect of propylene glycol after nasal administration. Their 13-week subchronic nose only inhalation study demonstrated that daily exposures to PG up to 5 mg/L for 6 h/day did not induce biologically meaningful adverse effects in rats (Langston et al., 2021).

3.2. Characterization of MX-loaded nanoemulsions

The characterization of the MX-NE1–4 nanoemulsion formulations was performed via DLS measurements, determination of encapsulation efficiency and the pH of these nasal formulations. The measured parameters can be found in Table 4.

Based on the DLS measurements, it can be claimed that the nanoemulsion formulations met the criteria of a nano drug delivery system. Their droplet size is below 300 nm and the PdI values are lower than 0.3 meaning that the droplet size distribution is monodisperse and the formulations contain MX in uniform size. MX-NE1 and MX-NE3 showed significantly lower ($p < 0.05$) droplet size in comparison to MX-NE2 and MX-NE4, which can be explained with the different ethanol content. Increasing the ethanol content beside the permanent surfactant concentration tends to further decrease the interfacial tension, which results in droplet size reduction (Wang et al., 2020). The surface charge of the formulations expressed as zeta potential is negative. It is recommended for a nasal delivery system to have a slightly negative surface charge, as this enhances the nasal absorption through the nasal mucosa. The high encapsulation efficiency value (above 60%) is a requirement to ensure that a proper dosing can occur via high drug loading. The pH values of the formulations are within the nasal conditions (pH 5.3 to 6.5) which means that no further pH-setting additives are needed to ensure that the nasal formulation is not irritative inside the nasal cavity.

3.3. Rheological characterization

3.3.1. Viscosity of the nanoemulsions

As the reference for viscosity measurements, the rheological properties of 0.5% w/w hyaluronic acid (HA) solution, as a frequently applied viscosity enhancer in nasal and ocular formulations, were compared to our nanoemulsions. The viscosity values can be seen in Table 5.

Statistical significance of viscosity results was determined using the paired *t*-test. Changes were considered statistically significant at $p < 0.05$. The viscosity of MX-NE1 and MX-NE3 formulations is significantly higher, than that of MX-NE2, MX-NE4 and HA solution. The viscosity difference can be explained with the different amount of ethanol. Increasing the ethanol content tends to increase the dynamic viscosity. This phenomenon can be explained with different droplet size and thus the rigid nature of smaller droplets. Larger droplets are nonrigid and

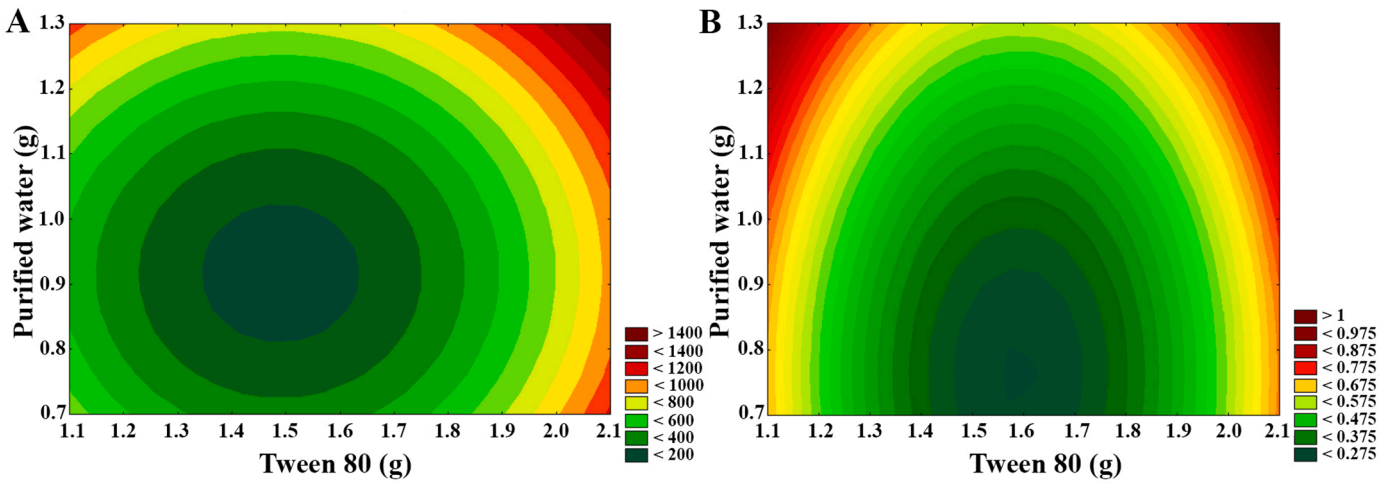

Fig. 1. 2D surface plots of the Box-Behnken factorial design: the effect of the amount of Tween 80 and purified water on droplet size (A) and polydispersity index (B).

Table 3
Composition of the investigated MX-NE1–4 nanoemulsion formulations.

	MX-NE1	MX-NE2	MX-NE3	MX-NE4
Tween 80 (g (% w/w))	1.50 (33.04)	1.50 (35.47)	1.50 (30.93)	1.50 (38.29)
Ethanol (g (% w/w))	1.30 (28.64)	0.70 (16.55)	1.30 (26.81)	0.70 (17.87)
Propylene glycol (g (% w/w))	0.70 (15.42)	1.00 (23.65)	1.00 (20.62)	0.70 (17.67)
Purified water (g (% w/w))	0.90 (19.83)	0.90 (21.28)	0.90 (18.56)	0.90 (22.97)
Castor oil (g (% w/w))	0.13 (2.86)	0.12 (2.84)	0.14 (2.89)	0.11 (2.81)
MX (mg (% w/w))	9.06 (0.2)	8.44 (0.2)	9.68 (0.2)	7.82 (0.2)

Table 4
Droplet size, polydispersity index, zeta potential, encapsulation efficiency and pH value of the selected nanoemulsion formulations. Results are presented as means ± SD ($n = 3$).

	Droplet size (nm)	PdI	zeta potential (mV)	EE%	pH
MX-NE1	150.5 ± 7.3	0.271 ± 0.026	−7.9 ± 1.9	63.7 ± 2.4	5.71 ± 0.2
MX-NE2	231.5 ± 9.1	0.236 ± 0.017	−10.8 ± 1.3	78.1 ± 4.1	5.49 ± 0.1
MX-NE3	158.5 ± 6.4	0.211 ± 0.023	−11.2 ± 1.5	79.2 ± 3.9	5.63 ± 0.1
MX-NE4	257.4 ± 8.6	0.268 ± 0.041	−8.3 ± 1.7	62.1 ± 3.0	5.78 ± 0.3

Table 5
Viscosity values of the MX-NE1–4 nanoemulsion formulations and the 0.5% w/w HA solution.

Sample	Viscosity (mPa × s)
MX-NE1	105.05 ± 1.15
MX-NE2	42.29 ± 3.32
MX-NE3	121.18 ± 4.99
MX-NE4	40.03 ± 2.83
0.5% w/w HA solution	158.18 ± 7.31

deformable, showing a different rheological behavior. Emulsions of deformable particles exhibit both shear thinning and elastic effects (normal stresses), even at low dispersed-phase concentrations, however, the viscosity shows an opposite trend; it increases with the decrease in droplet size (Pal, 1996). Low viscosity values indicate higher drug release as the drug can transfer more efficiently from the system to the dissolution media without the restricting effect of the carrier. Low viscosity nasal formulations are also favourable considering the mucociliary activity. Highly viscous systems can inhibit the ciliary activity in a manner which can affect the physiological elimination mechanisms. By decreasing the viscosity, a more natural and ciliary friendly application can be obtained.

3.3.2. *Mucoadhesion study*

Mucoadhesion is of particular importance for nasal nanocarriers, as increasing the residence time in the nasal cavity increases the potential for absorption by allowing the drug to remain on the nasal mucosa. During the tensile test, 0.5% w/w HA solution was used as the reference as it is known to have satisfactory mucoadhesive properties when applied nasally (Horvát et al., 2009). It can be claimed that all MX-NE formulations exceeded the adhesive force and the adhesive work of the HA solution, meaning that the total mucoadhesion is higher. However, they showed lower viscosity, which predicts further advantages in maintaining physiological ciliary activity. The results were evaluated statistically as well, using one-way ANOVA with post-hoc Tukey's multiple comparison test. All MX-NE formulations had significantly higher adhesive markers, among them the MX-NE3 formulation had the highest adhesive work, which refers to the integrated mucoadhesion of a specific formulation. With these results (Fig. 2), it can be claimed that the formation of nanoemulsion with high negative zeta potential will result in significant mucoadhesiveness, which enables a permeation for a prolonged time period as they are more resistant against the elimination mechanisms of mucociliary clearance.

3.3.3. *Spreading properties via contact angle measurement*

Proper spreading on biological surfaces, particularly on the hydrophobic nasal mucosa is of paramount importance. By measuring the contact angles of the optimized nanoemulsion formulations (MX-NE1–4) against a purely hydrophobic surface (solid paraffin film), a proper spreading tendency was experienced. Generally, the spreading mechanism of surfactants over hydrophobic surfaces can be described as a slow transfer of the surfactant molecules onto the bare hydrophobic surfaces in front of the moving liquid (Lee et al., 2008). This phenomenon can be seen with the rapidly decreasing contact angle values in Fig. 3. With quick spreading, a higher surface of the nasal mucosa can be covered with the nanoemulsions predicting improved drug release and absorption profile.

3.4. *Stability studies*

Physical stability refers to the permanence of droplet size and droplet

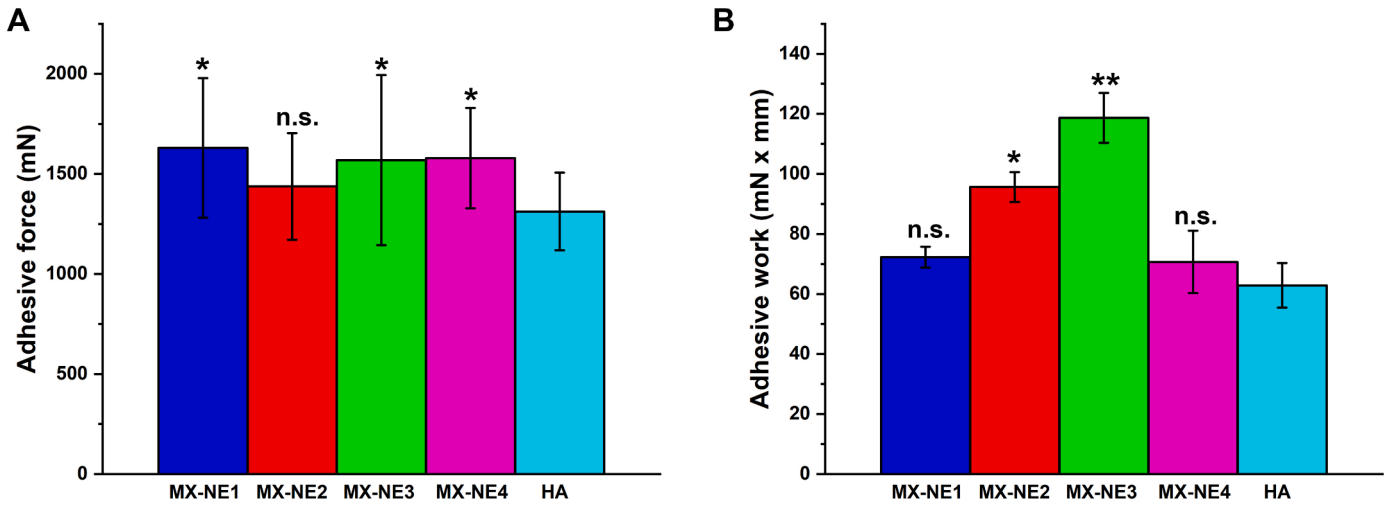

Fig. 2. Adhesive work of the MX-NE1–4 formulations compared to 0.5% w/w HA solution. The results are expressed as means ± SD ($n = 5$). Statistical analysis: Tukey's multiple comparison test (n.s. $p > 0.05$, * $p < 0.05$, ** $p < 0.01$).

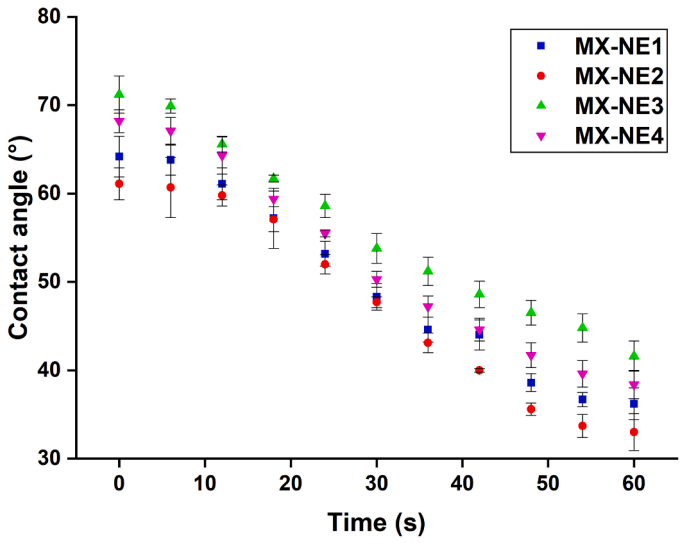

Fig. 3. Contact angles of the optimized MX-loaded nanoemulsion formulations (MX-NE1–4) plotted against time. The results are expressed as average ± SD ($n = 3$).

size distribution through storage. The formulations were stored at ambient temperature (25 °C) for 4 weeks and the measurements were carried out on every 7th day. The formulations remained stable and under the criteria limits of droplet size and PdI during the whole measurement, which indicates high stability. No visible separation was experienced. Dilution stability refers to the constancy of droplet size and droplet size distribution when the nanocarrier is faced against volume expansion and concentration decrease. Dilution stability is an important parameter in mimicking the physiological dilution process after nasal administration of the prepared nanoemulsions. If the system is maintaining physical stability, as it can be observed in the case of the MX-NE1–4 nanoformulations, the appearance remains transparent and the droplet size will be constant, which will allow uniform drug release as well as absorption profile during the administration. The droplet size slightly decreased, whilst the PdI slightly increased. It can be explained by the fact that the lower the concentration is, the bigger the distance is between each droplet. Consequently, a tendency can be observed to individual droplet formation which may vary in size and size distribution. The results can be seen in Figs. 4 and 5.

3.5. *In vitro nasal applicability study*

3.5.1. *In vitro nasal dissolution study and statistical analysis*

The *in vitro* drug release profiles of the MX-NE1–4 nanoemulsion formulations compared to the initial MX (suspended with SNES) can be seen in Fig. 5. Based on the curves, it can be concluded that the nanoemulsions allow a higher dissolution rate compared to the initial MX. Drug release from the system may be more inhibited in case of nanoemulsions, however, the achievement of the nano size range and its homogenous droplet size distribution led to a higher degree of release under nasal conditions. Besides the nano size range, the proper mucoadhesive properties allow higher residence time on the nasal mucosa which also benefit the release of drug per time period. The MX-NE1 and MX-NE3 formulations showed higher drug release which can be explained by the droplet size difference in comparison to the other two formulations, i.e. their lower droplet size facilitates the drug transport across the membrane used.

Model-independent statistical kinetics is a great tool to compare different formulations. The main calculated parameters were the following: percentage dissolution efficiency, mean dissolution time and relative dissolution. The 15-min measurement point was appointed for comparison as it is the average residence time on the nasal mucosa. The calculated parameters can be seen in Table 6.

3.5.2. *In vitro nasal diffusion study*

To simulate the absorption from the nasal cavity to the blood vessels, an *in vitro* nasal diffusion study was performed using a modified horizontal diffusion cell. The cumulative permeability values were calculated from the measured concentrations via HPLC. In Fig. 6 the same tendency can be observed as from the dissolution study, where the permeated drug amount is higher in case of the MX-NE1–4 formulations compared to the initial MX. The same tendency can be experienced among the formulations as in case of the drug release study. The MX-NE3 formulation prevailed in the *in vitro* nasal diffusion study, which can be claimed with the low droplet size, with the highest encapsulation efficiency and mainly with the remarkable penetration enhancer effect due to the highest propylene glycol content compared to other formulations.

The calculated flux and permeability coefficient values can be seen in Table 7. The results can be explained by the monodisperse nano size range, which allows uniform and higher permeability across membranes compared to the macro sized ranged initial MX.

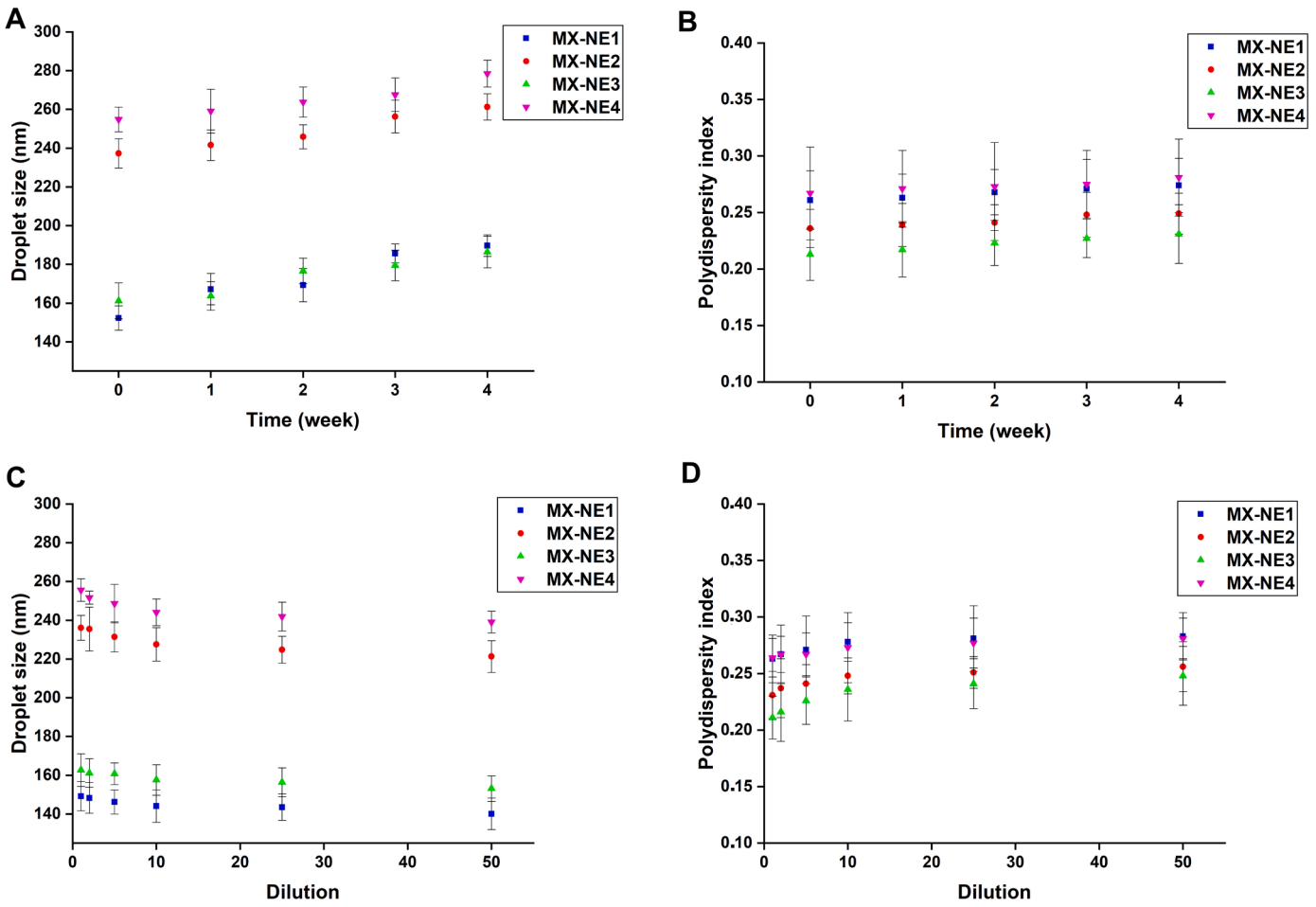

Fig. 4. Droplet size (A) and droplet size distribution (PdI) (B) values of the MX-NE1–4 nanoemulsion formulations during physical stability investigation. Results are expressed as means ± SD ($n = 3$).

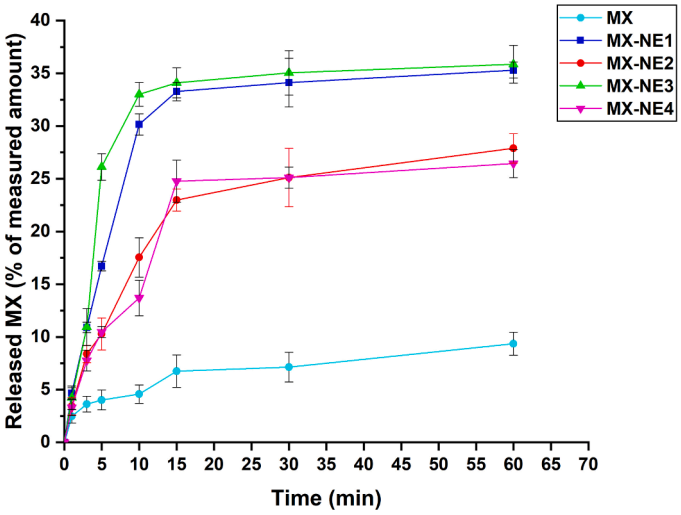

Fig. 5. *In vitro* drug release of MX-NE1–4 formulations compared to the initial MX at nasal conditions (SNES, 35 °C) from dialysis bags with 12–14 kD MWCO. The results are expressed as means ± SD ($n = 3$).

3.5.3. *In vitro cytotoxicity assay*

MTT assay was performed on NIH/3T3 mouse embryonic fibroblast cells to investigate the cytotoxic effect of MX nanoemulsions in comparison to initial MX. Based on the measured inhibition values (Fig. 7), no significant difference ($p > 0.05$ at all levels) was experienced between MX nanoemulsions and initial MX. MX is a highly tolerable API even in higher dosages, therefore the nanoemulsion formulations can be safely applied intranasally with a minimal risk of nasal mucosa irritation.

Table 6
Dissolution efficiency (%DE), mean dissolution time (MDT) and relative dissolution ($RD_{15\ min}$) of the MX-NE1–4 nanoemulsion formulations compared to MX. Data are based on the average of the parallel drug release curves.

Sample	%DE	MDT (min)	$RD_{15\ min}$
MX	4.14	35,36	1.00
MX-NE1	54.32	17.14	13.121
MX-NE2	49.67	17.89	11.996
MX-NE3	61.12	16.64	14.763
MX-NE4	46.15	17.79	11.147

4. Conclusions

In conclusion, 4 different nanoemulsion formulations were compared to determine the most suitable composition for nasal application. The nano size range in monodisperse distribution contributed to the high permeability and drug release of MX. The most appropriate rheological characteristics were acquired in case of MX-NE3 formulation with adequate wettability on hydrophobic surface, the highest mucoadhesion and the lowest viscosity which helps with the easy application. The low viscosity also promotes that the MX-NE3 formulation can be used in a nasal spray as well. These factors contributed to

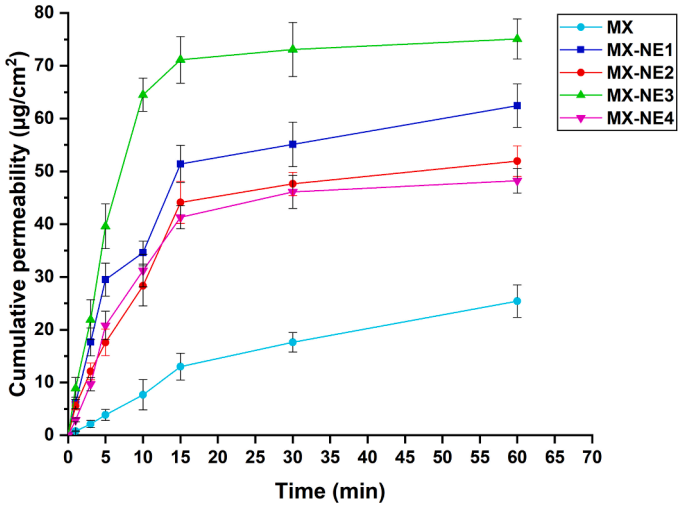

Fig. 6. *In vitro* nasal diffusion study of MX-NE1-4 formulations compared to the initial MX. The results are expressed as means ± SD ($n = 3$).

Table 7
Flux (J) and permeability coefficient (K_p) of the MX-NE1–4 nanoemulsion formulations compared to the initial MX. Data are based on the average of the parallel drug release curves.

Sample	J (μg/cm²)	K_p (cm/h)
MX	25.41	0.1143
MX-NE1	62.46	0.2811
MX-NE2	51.94	0.2337
MX-NE3	75.08	0.3379
MX-NE4	48.21	0.2811

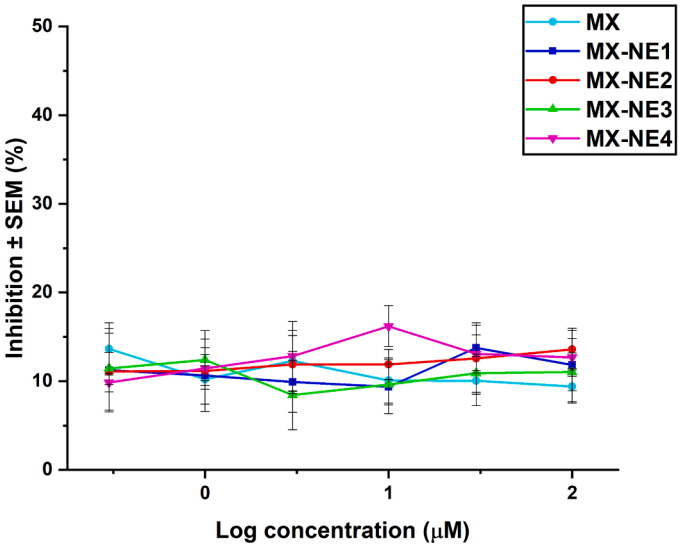

Fig. 7. Antiproliferative MTT assay of MX compared with the MX-NE1–4 nanoemulsion formulations. Inhibition ± SEM (%) is presented as a function of log concentration (μM). Results are expressed as means ± SD ($n = 5$).

the highest drug release and permeability at nasal conditions. A significant cytotoxic effect of this formulation was also not observed compared to the initial MX.

Overall, MX-NE3 nanoemulsion formulation is recommended to be applied intranasally to deliver a more efficient concentration of API to the blood stream with rapid onset of action and the protection from the gastrointestinal degradation metabolisms.

Funding

The publication was funded by The University of Szeged Open Access Fund (FundRef, Grant No. 5638).

CRediT authorship contribution statement

Bence Sipos: Conceptualization, Methodology, Software, Formal analysis, Investigation, Data curation, Writing – original draft, Visualization, Project administration. **Ildikó Csóka:** Conceptualization, Methodology, Validation, Formal analysis, Resources, Writing – review & editing, Supervision, Project administration. **Nimród Szivacski:** Software, Investigation, Writing – original draft. **Mária Budai-Szűcs:** Conceptualization, Resources, Investigation, Writing – original draft. **Zsuzsanna Schelcz:** Software, Investigation, Writing – original draft. **István Zupkó:** Conceptualization, Validation, Resources, Writing – review & editing, Project administration. **Piroska Szabó-Révész:** Methodology, Validation, Formal analysis, Writing – review & editing. **Balázs Volk:** Writing – review & editing, Resources. **Gábor Katona:** Conceptualization, Methodology, Validation, Formal analysis, Resources, Writing – review & editing, Supervision, Project administration.

Declaration of Competing Interest

The authors declare no conflict of interest.

Acknowledgments

This work was supported by the National Research, Development, and Innovation Office, Hungary (Richter-GINOP-2.2.1-15-2016-00007), and by Project No. TKP2021-EGA-32 was implemented with support provided by the Ministry of Innovation and Technology of Hungary from the National Research, Development and Innovation Fund, financed under the TKP2021-EGA funding scheme.

References

Bartos, C., Ambrus, R., Kovács, A., Gáspár, R., Sztojkov-Ivanov, A., Márki, Á., Janáky, T., Tamási, F., Kecskeméti, G., Szabó-Révész, P., 2018. Investigation of absorption routes of meloxicam and its salt form from intranasal delivery systems. Molecules 23, 1–13. https://doi.org/10.3390/molecules23040784.

Bonferoni, M.C., Rossi, S., Sandri, G., Ferrari, F., Gavini, E., Rassu, G., Giunchedi, P., 2019. Nanoemulsions for "nose-to-brain" drug delivery. Pharmaceutics 11, 1–17. https://doi.org/10.3390/pharmaceutics11020084.

Chou, T.H., Nugroho, D.S., Chang, J.Y., Cheng, Y.S., Liang, C.H., Deng, M.J., 2021. Encapsulation and characterization of nanoemulsions based on an anti-oxidative polymeric amphiphile for topical apigenin delivery. Polymers (Basel) 13. https://doi.org/10.3390/polym13071016.

Choudhury, H., Zakaria, N.F.B., Tilang, P.A.B., Tzeyung, A.S., Pandey, M., Chatterjee, B., Alhakamy, N.A., Bhattamishra, S.K., Kesharwani, P., Gorain, B., Md, S., 2019. Formulation development and evaluation of rotigotine mucoadhesive nanoemulsion for intranasal delivery. J. Drug Deliv. Sci. Technol. 54, 101301 https://doi.org/10.1016/j.jddst.2019.101301.

Espinoza, L.C., Vacacela, M., Clares, B., Garcia, M.L., Fabrega, M.J., Calpena, A.C., 2018. Development of a nasal donepezil-loaded microemulsion for the treatment of alzheimer's disease: *in vitro* and *ex vivo* characterization. CNS Neurol. Disord. Drug Targets 17, 43–53. https://doi.org/10.2174/1871527317666180104122347.

Gao, M., Mei, D., Huo, Y., Mao, S., 2019. Effect of polysorbate 80 on the intranasal absorption and brain distribution of tetramethylpyrazine phosphate in rats. Drug Deliv. Transl. Res. 9, 311–318. https://doi.org/10.1007/s13346-018-0580-y.

Horvát, S., Fehér, A., Wolburg, H., Sipos, P., Veszelka, S., Tóth, A., Kis, L., Kurunczi, A., Balogh, G., Kürti, L., Eros, I., Szabó-Révész, P., Deli, M.A., 2009. Sodium hyaluronate as a mucoadhesive component in nasal formulation enhances delivery of molecules to brain tissue. Eur. J. Pharm. Biopharm. 72, 252–259. https://doi.org/10.1016/j.ejpb.2008.10.009.

Horváth, T., Ambrus, R., Völgyi, G., Budai-Szűcs, M., Márki, Á., Sipos, P., Bartos, C., Seres, A.B., Sztojkov-Ivanov, A., Takács-Novák, K., Csányi, E., Gáspár, R., Szabó-Révész, P., 2016. Effect of solubility enhancement on nasal absorption of meloxicam. Eur. J. Pharm. Sci. 95, 96–102. https://doi.org/10.1016/j.ejps.2016.05.031.

Katona, G., Balogh, G.T., Dargó, G., Gáspár, R., Márki, Á., Ducza, E., Sztojkov-Ivanov, A., Tömösi, F., Kecskeméti, G., Janáky, T., Kiss, T., Ambrus, R., Pallagi, E., Szabó-Révész, P., Csóka, I., 2020. Development of meloxicam-human serum albumin nanoparticles for nose-to-brain delivery via application of a quality by design approach. Pharmaceutics 12, 97. https://doi.org/10.3390/pharmaceutics12020097.

Katona, G., Sipos, B., Budai-Szűcs, M., Balogh, G.T., Veszelka, S., Grósf, I., Deli, M.A., Volk, B., Szabó-Révész, P., Csóka, I., 2021. Development of *in situ* gelling meloxicam-human serum albumin nanoparticle formulation for nose-to-brain application. Pharmaceutics 13, 646. https://doi.org/10.3390/pharmaceutics13050646.

Langston, T., Randazzo, J., Kogel, U., Hoeng, J., Martin, F., Titz, B., Guedj, E., Schneider, T., Prabhakar, B., Zhang, J., Oldham, M., Lee, K., 2021. Thirteen-week nose-only inhalation exposures of propylene glycol aerosols in Sprague Dawley rats with a lung systems toxicology analysis. Toxicol. Res. Appl. 5, 239784732110210 https://doi.org/10.1177/23978473211021072.

Lee, K.S., Ivanova, N., Starov, V.M., Hilal, N., Dutschk, V., 2008. Kinetics of wetting and spreading by aqueous surfactant solutions. Adv. Colloid Interface Sci. 144, 54–65. https://doi.org/10.1016/j.cis.2008.08.005.

Marzuki, N.H.C., Wahab, R.A., Hamid, M.A., 2019. An overview of nanoemulsion: concepts of development and cosmeceutical applications. Biotechnol. Biotechnol. Equip. 33, 779–797. https://doi.org/10.1080/13102818.2019.1620124.

Pal, R., 1996. Effect of droplet size on the rheology of emulsions. AIChE J. 42, 3181–3190. https://doi.org/10.1002/aic.690421119.

Parepally, J.M.R., Mandula, H., Smith, Q.R., 2006. Brain uptake of nonsteroidal anti-inflammatory drugs: ibuprofen, flurbiprofen, and indomethacin. Pharm. Res. 23, 873–881. https://doi.org/10.1007/s11095-006-9905-5.

Prasetyo, B.E., Karsono, Maruhawa, S.M., Laila, L., 2018. Formulation and physical evaluation of castor oil based nanoemulsion for diclofenac sodium delivery system. Res. J. Pharm. Technol. 11, 3861–3865. https://doi.org/10.5958/0974-360X.2018.00707.2.

Rao, J., McClements, D.J., 2013. Optimization of lipid nanoparticle formation for beverage applications: influence of oil type, cosolvents, and cosurfactants on nanoemulsion properties. J. Food Eng. 118, 198–204. https://doi.org/10.1016/j.jfoodeng.2013.04.010.

Sari, T.P., Mann, B., Kumar, R., Singh, R.R.B., Sharma, R., Bhardwaj, M., Athira, S., 2015. Preparation and characterization of nanoemulsion encapsulating curcumin. Food Hydrocoll. 43, 540–546. https://doi.org/10.1016/j.foodhyd.2014.07.011.

Shaker, D.S., Ishak, R.A.H., Ghoneim, A., Elhuoni, M.A., 2019. Nanoemulsion: a review on mechanisms for the transdermal delivery of hydrophobic and hydrophilic drugs. Sci. Pharm. 87, 17. https://doi.org/10.3390/scipharm87030017.

Singh, Y., Meher, J.G., Raval, K., Khan, F.A., Chaurasia, M., Jain, N.K., Chourasia, M.K., 2017. Nanoemulsion: concepts, development and applications in drug delivery. J. Control. Release 252, 28–49. https://doi.org/10.1016/j.jconrel.2017.03.008.

Sipos, B., Szabó-Révész, P., Csóka, I., Pallagi, E., Dobó, D.G., Bélteky, P., Kónya, Z., Deák, Á., Janovák, L., Katona, G., 2020. Quality by design based formulation study of meloxicam-loaded polymeric micelles for intranasal administration. Pharmaceutics 12, 1. https://doi.org/10.3390/pharmaceutics12080697.

Sipos, B., Csóka, I., Budai-Szűcs, M., Kozma, G., Berkesi, D., Kónya, Z., Balogh, G.T., Katona, G., 2021a. Development of dexamethasone-loaded mixed polymeric micelles for nasal delivery. Eur. J. Pharm. Sci. 166 https://doi.org/10.1016/j.ejps.2021.105960.

Sipos, B., Katona, G., Csóka, I., 2021b. A systematic, knowledge space-based proposal on quality by design-driven polymeric micelle development. Pharmaceutics 13. https://doi.org/10.3390/pharmaceutics13050702.

Szabó-Révész, P., 2018. Modifying the physicochemical properties of NSAIDs for nasal and pulmonary administration. Drug Discov. Today Technol. 27, 87–93. https://doi.org/10.1016/j.ddtec.2018.03.002.

Wang, Z., Liu, H., Zhang, Z., Sun, B., Zhang, J., Lou, W., 2020. Research on the effects of liquid viscosity on droplet size in vertical gas–liquid annular flows. Chem. Eng. Sci. 220, 115621 https://doi.org/10.1016/j.ces.2020.115621.